Scaling for gap plasmon based waveguides

Sergey I. Bozhevolnyi[1,2] **and Jesper Jung**[1]

[1]*Department of Physics and Nanotechnology, Aalborg University, Skjernvej 4A, DK-9220 Aalborg Øst, Denmark*
[2]*Institute of Sensors, Signals and Electrotechnics (SENSE), University of Southern Denmark, Niels Bohrs Allé 1, DK-5230 Odense M, Denmark*
seib@sense.sdu.dk

Abstract: Using the effective-index approach and an explicit expression for the propagation constant of gap surface plasmon polaritons (G-SPPs) obtained for moderate gap widths, we introduce a normalized waveguide parameter characterizing the mode field confinement and obtain the corresponding expressions for various (gap, trench and V-groove) G-SPP based waveguides. Usage of the obtained relations is investigated with a finite-element method, demonstrating that waveguides with different dimensions and operating at different wavelengths, but having the same normalized parameter, exhibit very similar field confinement. These relations allow one to design G-SPP waveguides for single-mode operation supporting a well-confined fundamental mode.

OCIS codes: (240.6680) Surface plasmons; (230.7380) Waveguides, channeled ; (250.5300) Photonic integrated circuits

References and links

1. H. Raether, *Surface Plasmons* (Springer-Verlag, Berlin, 1988).
2. E. N. Economou, "Surface plasmons in thin films," Phys. Rev. **182**, 539-554 (1969).
3. S. I. Bozhevolnyi, "Effective-index modeling of channel plasmon polaritons," Opt. Express **14**, 9467-9476 (2006).
4. K. Tanaka and M. Tanaka, "Simulations of nanometric optical circuits based on surface plasmon polariton gap waveguide," Appl. Phys. Lett. **82**, 1158-1160 (2003).
5. K. Tanaka, M. Tanaka, and T. Sugiyama, "Simulation of practical nanometric optical circuits based on surface plasmon polariton gap waveguides," Opt. Express **13**, 256-266 (2005).
6. S. H. Chang, T. C. Chiu, and C.-Y. Tai, "Propagation characteristics of the supermode based on two coupled semi-infinite rib plasmonic waveguides," Opt. Express **15**, 1755-1761 (2007).
7. I. V. Novikov and A. A. Maradudin, "Channel polaritons," Phys. Rev. B **66**, 035403 (2002).
8. D. K. Gramotnev and D. F. P. Pile, "Single-mode subwavelength waveguide with channel plasmon-polaritons in triangular grooves on a metal surface," Appl. Phys. Lett. **85**, 6323-6325 (2004).
9. S. I. Bozhevolnyi, V. S. Volkov, E. Devaux, and T. W. Ebbesen, "Channel plasmon-polariton guiding by subwavelength metal grooves," Phys. Rev. Lett. **95**, 046802 (2005).
10. S. I. Bozhevolnyi, V. S. Volkov, E. Devaux, J.-Y. Laluet, and T. W. Ebbesen, "Channel plasmon subwavelength waveguide components including interferometers and ring resonantors," Nature **440**, 508-511 (2006).
11. V. S. Volkov, S. I. Bozhevolnyi, E. Devaux, J.-Y. Laluet, and T. W. Ebbesen, "Wavelength selective nanophotonic components utilizing channel plasmon polaritons," Nano Lett. **7**, 880-884 (2007).
12. E. Moreno, F. J. Garcia-Vidal, S. G. Rodrigo, L. Martin-Moreno, and S. I. Bozhevolnyi, "Channel plasmon-polaritons: modal shape, dispersion, and losses," Opt. Lett. **31**, 3447-3449 (2006).
13. G. B. Hocker and W. K. Burns, "Mode dispersion in diffused channel waveguides by the effective index method," Appl. Opt. **16**, 113-118 (1977).
14. A. Boltasseva, T. Nikolajsen, K. Leosson, K. Kjaer, M. S. Larsen, and S. I. Bozhevolnyi, "Integrated optical components utilizing long-range surface plasmon polaritons," J. Lightwave Technol. **23**, 413-422 (2005).
15. R. Zia, A. Chandran, and M. L. Brongersma, "Dielectric waveguide model for guided surface polaritons," Opt. Lett. **30**, 1473-1475 (2005).
16. H. Kogelnik and V. Ramaswamy, "Scaling rules for thin-film optical waveguides," Appl. Opt. **13**, 1857-(1974).
17. S. I. Bozhevolnyi, V. S. Volkov, E. Devaux, J.-Y. Laluet, and T. W. Ebbesen, "Channelling surface plasmons," Appl. Phys. A **89**, 225-231 (2007).
18. E. D. Palik, *Handbook of Optical Constants of Solids* (Academic, New York, 1985).

#90643 - $15.00 USD Received 11 Dec 2007; revised 7 Feb 2008; accepted 7 Feb 2008; published 12 Feb 2008

19. M. Yan and M. Qiu, "Guided plasmon polariton at 2D metal corners," J. Opt. Soc. Am. B **24**, 2333-2342 (2007).

1. Introduction

Photonic components are superior to electronic ones in terms of operational bandwidth but suffer from the diffraction limit that constitutes a major problem on the way towards miniaturization and high density integration of optical circuits. The degree of light confinement in dielectric structures, including those based on the photonic band-gap effect, is fundamentally limited by the light wavelength in the dielectric used. The main approach to circumvent this problem is to take advantage of the hybrid nature of surface plasmon polaritons (SPPs) whose subwavelength confinement is achieved due to the very short (nanometer-sized) penetration of light in metals [1]. The important issue in this context is to strongly confine the SPP field in the cross section perpendicular to the SPP propagation direction (smaller cross sections ensure smaller bend losses and higher densities of components), while keeping relatively low propagation loss. Among various SPP guiding configurations, waveguides utilizing SPP modes supported by a dielectric gap between two metal surfaces [2] promise the possibility of achieving a better trade-off between the lateral confinement and the propagation loss [3]. Gap-SPP (G-SPP) based configurations include waveguides having the gap width varying in the lateral direction [4, 5], trench [3, 6] and V-groove [7-9] waveguides. The latter configuration has recently been exploited to realize various subwavelength waveguide components, including Mach-Zehnder interferometers and waveguide-ring resonators [10] as well as add-drop multiplexers and grating filters [11].

Modeling of SPP waveguides allowing for the two-dimensional (2D) mode field confinement (in the cross section perpendicular to the propagation direction) is, in general, a rather complicated problem requiring the usage of sophisticated computational techniques [4-6, 7, 8, 12], which is often time-consuming due to the very detailed discretization required near metal edges. Even though very careful and detailed simulations are crucial for understanding intricate physical phenomena involved (e.g., hybridization of channel and wedge SPP modes [12]), it has been found that the effective-index method (EIM) [13] can be quite helpful in judging upon the existence of guided (bound) SPP modes [3, 9, 14, 15]. The main attractive feature of the EIM is that it allows one to combine the results of modeling conducted for one-dimensional (1D) waveguide configurations so that the characteristics of 2D (channel) waveguides can be described [13]. For a rectangular-core waveguide, one should first analyze a planar (slab) waveguide obtained by letting one dimension of the original 2D waveguide approach infinity. The obtained in this way mode propagation constant(s) is then used to define the corresponding effective dielectric index(es) assigned to the core index(es) of another 1D waveguide considered in the perpendicular direction. The propagation constant(s) of this second waveguide are taken to represent those of the original rectangular waveguide [13]. Furthermore, for the purpose of evaluating the guiding potential one can make use of the normalized waveguide parameter (normalized frequency [16]) avoiding the implementation of the second step in the EIM [3]. Note that the waveguide parameter can be rigorously introduced only for 1D (thin-film) waveguide configurations [16], and that its usage for 2D SPP-based waveguides should thus be carefully examined.

In this work, using the EIM along with an explicit (approximate) expression for the G-SPP propagation constant obtained for moderate gap widths, we introduce a normalized waveguide parameter characterizing the mode field confinement and obtain the corresponding expressions for various (gap, trench and V-groove) G-SPP based waveguides. Usage of the obtained relations is investigated with a finite-element method (FEM), demonstrating that waveguides with different dimensions and operating at different wavelengths, but having the same normalized parameter, exhibit very similar field confinement. These exceedingly simple relations allow one to properly choose the system parameters in a broad range so as to realize the single-mode operation of G-SPP waveguides with a well-confined fundamental mode.

#90643 - $15.00 USD Received 11 Dec 2007; revised 7 Feb 2008; accepted 7 Feb 2008; published 12 Feb 2008

2. G-SPP propagation constant for moderate gap widths

Many different SPP modes can be found in multiple-interface systems [2], when the SPPs associated with individual metal-dielectric interfaces start interacting with each other. Considering the SPP modes associated with two metal-dielectric interfaces one finds that the SPP modes can be guided within a thin dielectric layer surrounded by metals (i.e. inside a gap between metals), constituting (for even symmetry of the transverse field component) G-SPP modes that can be found for *any gap* width [2-4]. The G-SPP characteristics were discussed in detail elsewhere [17], paying special attention to the non-trivial dependence of the G-SPP propagation length on the gap width that indicates that G-SPPs exploit in the most efficient way the available dielectric space (gap) between the metal walls minimizing thereby the absorption loss [3]. This remarkable feature stimulates investigations of various G-SPP based waveguide geometries. Since the G-SPP effective index is strongly dependent on the gap width (increasing with its decrease) it is natural to exploit this dependence for achieving the 2D lateral mode confinement by laterally varying the gap width forming gap [4, 5], trench [3, 6] and V-groove [7-9] waveguides (Fig. 1). In general, guided modes in all these configurations are laterally confined to a dielectric space between the *closest* metal surfaces, where the G-SPP effective index reaches its largest value, i.e. to a gap [Fig. 1(a)], in a trench [Fig. 1(b)] or to the bottom of a V-groove [Fig. 1(c)]. In the EIM, the corresponding waveguide modes can be evaluated by considering a 1D multilayer structure whose layers feature the refractive indexes associated with the relevant G-SPP modes [3].

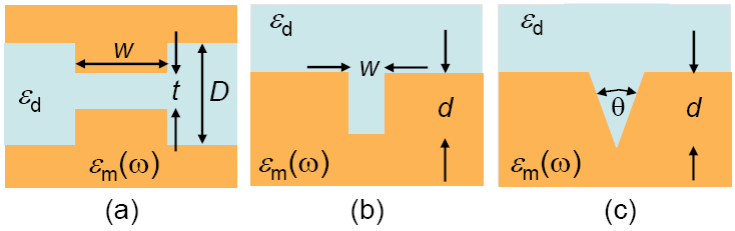

Fig. 1. Schematic of the G-SPP based waveguides under consideration.

For the purpose of obtaining simple design guidelines, we start with deriving an explicit expression for the G-SPP propagation constant that can be used for moderate gap widths. Applying the appropriate boundary conditions for the electric field components and the aforementioned field symmetry, allows one to obtain the G-SPP dispersion relation [2]:

$$\tanh\left(k_z^{(d)}t/2\right)=-\left(\varepsilon_d k_z^{(m)}\right)/\left(\varepsilon_m k_z^{(d)}\right),\ \text{with}\ k_z^{(m,d)}=\sqrt{k_{gsp}^2-\varepsilon_{m,d}\,k_0^2}\ \text{and}\ k_0=\frac{2\pi}{\lambda}\ , \quad (1)$$

where t is the gap width, ε_d and ε_m are the dielectric constants of correspondingly dielectric and metal, and k_{gsp} denotes the propagation constant of the fundamental G-SPP mode with the transverse field component having the same sign across the gap. For sufficiently small gap widths ($t \to 0$), one can use the approximation $\tanh x \approx x$ resulting in the following expression:

$$k_{gsp} \approx k_0\sqrt{\varepsilon_d+0.5\left(k_{gsp}^0/k_0\right)^2+\sqrt{\left(k_{gsp}^0/k_0\right)^2\left[\varepsilon_d-\varepsilon_m+0.25\left(k_{gsp}^0/k_0\right)^2\right]}} \quad (2)$$

$$\text{with}\quad k_{gsp}^0=-\frac{2\varepsilon_d}{t\varepsilon_m}\ .$$

Here, k_{gsp}^0 represents the G-SPP propagation constant in the limit of vanishing gaps ($t \to 0$), for which the real part of the correspondent effective index, $\mathrm{Re}\{k_{gsp}\lambda/(2\pi)\}$, becomes much larger than the dielectric refractive index. At the same time, the imaginary part of the G-SPP

#90643 - $15.00 USD Received 11 Dec 2007; revised 7 Feb 2008; accepted 7 Feb 2008; published 12 Feb 2008

propagation constant increases rapidly as well, resulting in a decrease of the G-SPP propagation length. For our purpose, it is desirable to further simplify the small-gap approximation given by Eq. (2), which is somewhat cumbersome to handle. Considering different gap-width-dependent terms in Eq. (2), one notices that for not too small gaps, i.e. when $\left|k_{gsp}^{0}\right| < k_0 \Leftrightarrow t > (\lambda\varepsilon_d)/(\pi|\varepsilon_m|)$, it can be approximated as follows:

$$k_{gsp} \approx k_0 \sqrt{\varepsilon_d + \frac{2\varepsilon_d \sqrt{\varepsilon_d - \varepsilon_m}}{k_0 t(-\varepsilon_m)}} \quad . \tag{3}$$

The G-SPP characteristics were calculated for air gaps in gold for several wavelengths in the interval between visible and telecom wavelengths using the exact (implicit) dispersion relation [Eq. (1)] and the above explicit (analytic) formula (Fig. 2). The following dielectric constants of gold were used in the simulations: n = 0.166 + 3.15i (λ = 653 nm), 0.174 + 4.86i (775 nm), 0.272 + 7.07i (1033 nm), and 0.55 + 11.5i (1550 nm) [18].

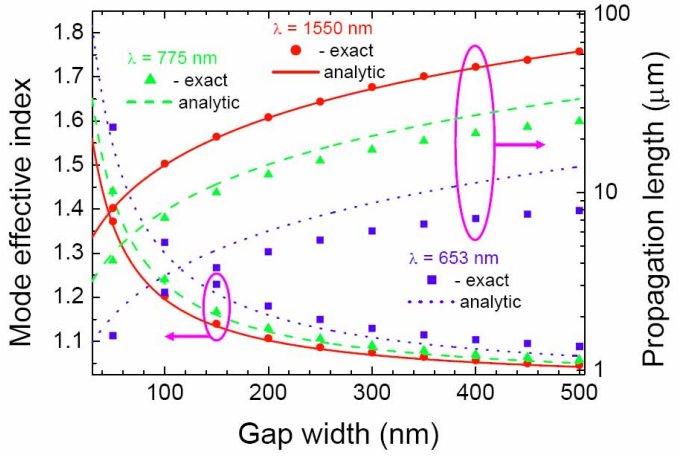

Fig. 2. The G-SPP mode effective index and its propagation length as a function of the width t of the air gap in gold for several light wavelengths calculated exactly [Eq. (1)] and using the analytic (moderate gap) approximation [Eq. (3)].

It is seen that the above approximation gives quite accurate values for both the G-SPP propagation length and effective index. In fact progressively more accurate values are obtained for longer wavelengths because of the large values of $|\varepsilon_m|$. Even for shorter wavelengths and other materials, the obtained relation is still fairly accurate. For example, considering the system parameters used for simulations of G-SPP waveguides [4], i.e. λ = 532 nm, ε_d = 1, Re(ε_m) ≅ - 12.6 (silver), t = 34 and 85 nm, results, when using Eq. (3), in effective G-SPP indexes N_{eff} ≅ 1.57 and 1.26, respectively. These values agree well with the values N_{eff} ≅ 1.61 and 1.28 obtained directly from the dispersion relation [4].

3. Gap waveguides

The lateral G-SPP mode confinement in gap waveguides [4, 5] is achieved by decreasing the gap within a stripe of width w [Fig. 1(a)]. The corresponding waveguide modes can be described within the EIM framework by considering TE (electric field is parallel to interfaces) modes in a *symmetric* three-layer structure whose refractive indexes are given by the appropriate G-SPP effective indexes [3]. The normalized waveguide parameter (normalized frequency [16]) of a symmetric optical waveguide, consisting of a film (core) with the thickness w and the refractive index n_1 embedded in a medium (cladding) with the refractive index n_2, is given by [16]:

#90643 - $15.00 USD Received 11 Dec 2007; revised 7 Feb 2008; accepted 7 Feb 2008; published 12 Feb 2008

$$V = w k_0 \sqrt{n_1^2 - n_2^2} \quad . \tag{4}$$

For the considered waveguide configuration [Fig. 1(a)], the core and cladding refractive indexes correspond to the effective indexes of G-SPP modes supported by gaps having the width t and D, accordingly. These indexes can be approximated using the explicit relation for the G-SPP propagation constant [Eq. (3)], resulting thereby in the following expression for the normalized waveguide parameter:

$$V_{gsp} \cong 2w \sqrt{\frac{\pi \varepsilon_d \sqrt{|\varepsilon_d - \varepsilon_m|}}{\lambda |\varepsilon_m|} \left(\frac{1}{t} - \frac{1}{D} \right)} \quad . \tag{5}$$

It is seen that this waveguide parameter depends explicitly on the light wavelength, reflecting the fact that the gap widths considered are relatively large. In the limit of very narrow gaps, i.e. when $t << (\lambda \varepsilon_d)/(\pi |\varepsilon_m|)$, the G-SPP propagation constant becomes equal to k_{gsp}^0 [Eq. (2)] and the wavelength dependence disappears as expected for SPP waveguides whose operation is not limited by diffraction. Note that the above condition is rather stringent requiring extremely narrow gaps. Thus, for example, a gap width t << 13 nm is required for the system parameters used in the aforementioned gap waveguide made of silver.

The usage of the waveguide parameter V allows one to choose the system parameters that ensure a well-confined fundamental mode. In fact, the design of single-mode waveguides is often aimed at achieving the best lateral mode confinement, because this confinement strongly influences the maximum density of waveguide components in integrated optical circuits [3]. For the fundamental TE_0 mode, there is no cutoff (with respect to the width w) in a symmetric waveguide, but the effective mode width diverges in the limit of both very wide ($w \to \infty$) and very narrow($w \to 0$) waveguides, reaching its minimum at $V_0 = 1.73$ [16]. The parameter space for the single-mode symmetric waveguide, within which the fundamental mode is well confined, can thereby be determined by the following unequality: $1.73 \le V \le \pi$ [16]. In order to illustrate the usage of the waveguide parameter we modeled (using the FEM and above dielectric constants) two different gap waveguides made of gold, operating at two different wavelengths, but characterized by the same waveguide parameter $V_{gsp} = 1.73$ (Fig. 3).

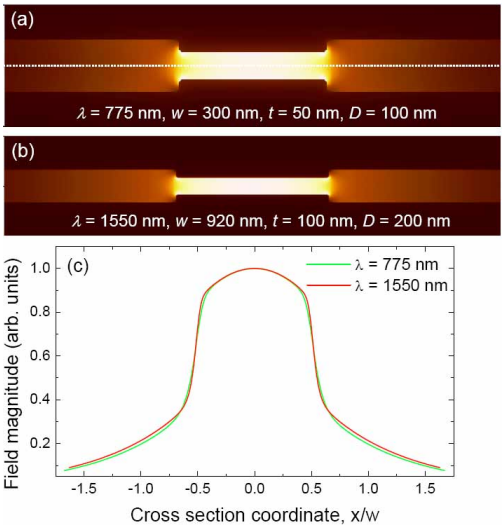

Fig. 3. (a, b). The G-SPP mode field magnitude distributions and (c) their lateral mid-plane cross sections shown by a dotted line in (a) for two waveguide configurations having the same waveguide parameter $V_{gsp} = 1.73$.

#90643 - $15.00 USD Received 11 Dec 2007; revised 7 Feb 2008; accepted 7 Feb 2008; published 12 Feb 2008

It is seen that the fundamental waveguide mode, when displayed using the normalized (with respect to the waveguide width w) cross section coordinate, exhibits the same confinement and field distribution in the lateral direction. All FEM simulations presented in this paper were conducted using the commercial software COMSOL with all sharp corners being rounded with a 10-nm radius, which is usually used in similar calculations [12, 19], and with the convergence achieved for a total number of unknowns in the range of $2{\cdot}10^5 - 4{\cdot}10^5$. The fact that the modes found for two rather different waveguide configurations exhibit such a striking similarity in their lateral distributions is related to the circumstance that the EIM, which was used to introduce the waveguide parameter [Eq. (5)], is quite accurate when applied to the gap waveguides [3]. Thus, for the considered configurations, the mode effective indexes calculated with the FEM, $N_{\mathrm{FEM}}(\lambda = 775\ \mathrm{nm}) \cong 1.365 + 0.014i$ and $N_{\mathrm{FEM}}(\lambda = 1550\ \mathrm{nm}) \cong 1.161 + 0.0080i$, are found being quite similar to those obtained with the EIM, $N_{\mathrm{EIM}}(\lambda = 775\ \mathrm{nm}) \cong 1.326 + 0.013i$ and $N_{\mathrm{EIM}}(\lambda = 1550\ \mathrm{nm}) \cong 1.145 + 0.0073i$.

4. Trench waveguides

The waveguide modes supported by rectangular trenches [Fig. 1(b)] can be described within the EIM framework by considering TE modes in a three-layer structure, in which a dielectric core, having the effective index of the corresponding G-SPP, is sandwiched between the air cladding and the gold substrate [3]. Using the approximation [Eq. (3)] of moderately narrow gaps (trenches) and the approach similar to that employed in the previous section, one obtains for the normalized waveguide parameter [16] of trench waveguides:

$$V_{tpp} \cong 2d\sqrt{\frac{\pi\,\varepsilon_d\sqrt{|\varepsilon_d - \varepsilon_m|}}{\lambda\, w|\varepsilon_m|}} \quad . \tag{6}$$

The trench SPP (TPP) mode fields decrease to (nearly) zero at the trench bottom because of the large magnitude of dielectric constant of the metal substrate and the boundary condition for the electric field [3]. For this reason, the TPP mode characteristics are nearly identical to the corresponding (odd) modes of the symmetrical gap waveguide having the double width, a circumstance that allows one to deduce a simple relation for the single-mode TPP guiding: $0.5\pi < V_{\mathrm{tpp}}(w, d) < 1.5\pi$ [3]. It is then reasonable to take as a compromise the waveguide parameter value $V_{\mathrm{tpp}} = \pi$ for the design of single-mode waveguides supporting a well-confined fundamental TPP mode. As in the previous case, we modeled two different trench waveguides characterized by the same waveguide parameter $V_{\mathrm{tpp}} = \pi$ (Fig. 4).

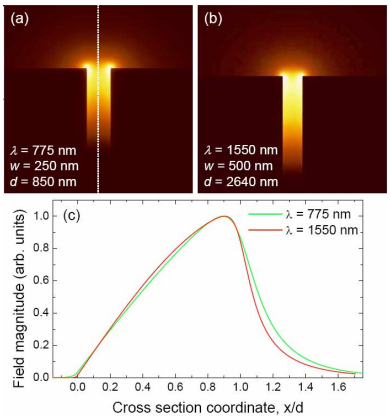

Fig. 4. (a, b). The TPP mode field magnitude distributions and (c) their lateral mid-plane cross sections shown by a dotted line in (a) for two waveguide configurations having the same waveguide parameter $V_{\mathrm{tpp}} = \pi$.

#90643 - $15.00 USD Received 11 Dec 2007; revised 7 Feb 2008; accepted 7 Feb 2008; published 12 Feb 2008

It is seen that the correspondence of the calculated TPP field magnitude distributions is rather good, albeit not as perfect as in the case of gap waveguides [cf. Figs. 4(c) and 3(c)]. We relate this fact to the circumstance that the correspondence between the EIM (approximate) simulations and accurate numerical modeling (e.g., when using the FEM) is generally worse for channel waveguides [12]. Thus, for the considered configurations, the mode effective indexes calculated with the FEM, $N_{\mathrm{FEM}}(\lambda = 775\ \mathrm{nm}) \cong 1.097 + 0.0050i$ and $N_{\mathrm{FEM}}(\lambda = 1550\ \mathrm{nm}) \cong 1.035 + 0.0022i$, are found to be quite different from those obtained with the EIM, $N_{\mathrm{EIM}}(\lambda = 775\ \mathrm{nm}) \cong 1.056 + 0.0037i$ and $N_{\mathrm{EIM}}(\lambda = 1550\ \mathrm{nm}) \cong 1.022 + 0.0018i$. It should be noted that the FEM modeling of the first trench waveguide (at $\lambda = 775$ nm) revealed the existence of an additional mode associated with the coupling of two wedge SPP modes that cannot be described within the EIM framework. The latter mode is very close to the cutoff (its effective index is larger than that of the corresponding SPP by only $\sim 7 \cdot 10^{-4}$) and therefore only weakly confined to the trench, extending in the lateral direction along the metal surface (away from each side of the trench) over several microns. We believe that, in practice, the existence of such a mode, whose characteristics are most strongly influenced by the curvature of wedges, can be disregarded.

5. V-groove waveguides

The SPP modes supported by metal grooves, in particular V-grooves [Fig. 1(c)], are conventionally called channel SPPs (CPPs) [7]. Careful analysis of CPP waveguides requires elaborate numerical modelling [7, 8, 12, 19], but the design guidelines can be worked out using the EIM [3, 9]. Within the framework of the EIM, one can find the CPP modes supported by a V-groove through analyzing a one-dimensional layered (in depth) guiding structure, in which a top layer of air and a bottom layer of metal abut a stack of layers having refractive indexes determined by the layer depth: the refractive index is equal to the G-SPP effective index for a gap width corresponding to the groove width at this depth [9]. The normalized CPP waveguide parameter can be obtained by integrating the index contrast over the groove depth, a straightforward procedure when using the moderate gap approximation [Eq. (3)] that results in the following expression:

$$V_{cpp} \cong 2\sqrt{\frac{k_0 d\, \varepsilon_d \sqrt{|\varepsilon_d - \varepsilon_m|}}{|\varepsilon_m| \tan(\theta/2)}} \quad . \tag{7}$$

It is seen that, since $\tan(\theta/2) = 0.5w/d$ (w being the groove width at the top of the groove), the CPP waveguide parameter is exactly twice that of TPP [Eq. (6)]: $V_{\mathrm{cpp}} = 2V_{\mathrm{tpp}}$. The latter relation is somewhat surprising as the cross section of a CPP waveguide is twice smaller than that of the TPP waveguide having the same width and depth [cf. Figs. 1(b) and 1(c)]. However, the G-SPP effective index increases with the decrease in the gap width and, thereby, *narrower* channels (trench and V-grooves) represent *stronger* waveguides (i.e., with larger waveguide parameters), as is also transparent from Eqs. (6) and (7), which accounts for the relation above. Note that the above relation for the CPP waveguide parameter [Eq. (7)] involves additional approximations as compared to Eq. (6). Thus, when using the EIM for CPP waveguides, it is implicitly assumed that the CPP electric field is polarized parallel to the sample surface, an approximation that can be justified only for narrow ($\theta << 1$) grooves [12]. Furthermore, when obtaining Eq. (7), the moderate gap approximation was applied for the gap widths varying all the way from 0 to the (maximum) groove width at the top of the groove.

Within the EIM framework, the CPP mode fields decrease to (nearly) zero at the groove bottom similarly to the TPP modes [3], and the single-mode CPP guiding should be, in principle, governed by the same condition as for the TPP guiding: $0.5\pi < V_{\mathrm{cpp}}(w, d) < 1.5\pi$. On the other hand, it has been noticed that the EIM *overestimates* the guiding capability of V-groove waveguides [12]. In the course of this work, we have also found that, contrary to the EIM simulations, the FEM modeling could not locate bound modes for the V-groove

#90643 - $15.00 USD Received 11 Dec 2007; revised 7 Feb 2008; accepted 7 Feb 2008; published 12 Feb 2008

waveguides characterized with a normalized waveguide parameter of π. On the other hand, the behavior of V-groove waveguides might still follow the *scaling* described by the waveguide parameter [Eq. (7)]. In order to asses this scaling, we modeled two different waveguides characterized with $V_{cpp}(w, d) = 1.34\pi$, a value which is still smaller than the cutoff value (1.5π) for the second mode (within the EIM framework). The two simulated CPP field magnitude distributions (of the fundamental modes) are shown in Fig. 5.

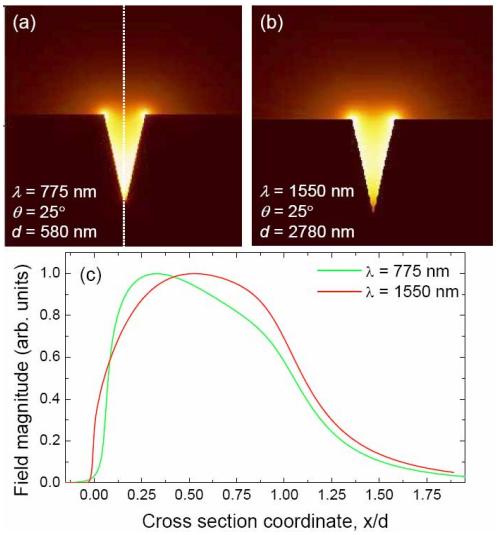

Fig. 5. (a, b). The CPP mode field magnitude distributions and (c) their lateral mid-plane cross sections shown by a dotted line in (a) for two waveguide configurations having the same waveguide parameter $V_{cpp} = 1.34\pi$.

It is seen that, even though the correspondence between the calculated CPP field magnitude distributions is worse than that found for the TPP distributions [cf. Figs. 5(c) and 4(c)], the CPP confinement to the groove region is rather similar for both configurations, with the major part of the CPP field being concentrated within the groove (i.e., for $0 \le x \le d$). The observed differences in the CPP distributions should be related to the aforementioned approximations introduced when applying the EIM and moderate gap approximation [Eq. (3)] for obtaining the CPP waveguide parameter. Influence of the EIM approximation is also reflected in the differences between the effective mode indexes calculated with the FEM, $N_{FEM}(\lambda = 775\text{ nm}) \cong 1.086 + 0.0074i$ and $N_{FEM}(\lambda = 1550\text{ nm}) \cong 1.012 + 0.0015i$, and those with the EIM, $N_{EIM}(\lambda = 775\text{ nm}) \cong 1.118 + 0.010i$ and $N_{EIM}(\lambda = 1550\text{ nm}) \cong 1.022 + 0.0023i$. It is in fact surprising that, despite all the approximations, the very simple formula obtained [Eq. (7)] reflects accurately enough the relations between the V-groove parameters that should be maintained in order to keep the same degree of CPP mode confinement. Finally, it is worth mentioning that the scaling established [Eqs. (5) – (7)] includes also the material dispersion, which is especially important for metals, resulting in the requirement of *progressively* wider (gap) or deeper (trench and V-groove) waveguides for longer wavelengths. Consequently, these waveguide configurations cannot be realized in the limit of ideal metals (when $\lambda \to \infty$), even though the G-SPP guiding does persist existing in this limit.

6. Conclusion

In summary, using the EIM along with an explicit expression for the G-SPP propagation constant obtained for moderate gap widths, we have obtained simple relations describing the normalized waveguide parameter for gap, trench and V-groove waveguides that characterizes the mode field confinement. Usage of the obtained relations was investigated with FEM simulations, demonstrating that waveguides with different dimensions and operating at

#90643 - $15.00 USD Received 11 Dec 2007; revised 7 Feb 2008; accepted 7 Feb 2008; published 12 Feb 2008

different wavelengths but having the same normalized parameter exhibit very similar field confinement. In the case of the gap waveguides, this confinement determines the lateral mode width, whereas for the TPP and CPP waveguides that are far from cutoff (which can be judged with the help of the corresponding waveguide parameters) the lateral mode width is simply set by the groove width *w* at the groove top. Note that it is the lateral mode width that governs both the bend loss and crosstalk between the neighbor waveguides, determining thereby the maximum density of waveguide components [3]. It should also be borne in mind that, as the TPP or CPP modes approach the cutoff and the mode fields become progressively larger at the groove edges, one should expect the occurrence of mode coupling to wedge SPP modes leading to their hybridization [12] that cannot be described with the EIM. These (sub-critical) waveguides are therefore outside the validity domain for the introduced waveguide parameter. However, the obtained expressions for the normalized waveguide parameter can still be used as *practical guidelines* to design G-SPP based gap, trench and V-groove waveguides for operation within a given wavelength range, so as to ensure the single-mode operation with a well-confined fundamental mode being far away from the cutoff. The latter is very important not only for minimizing the lateral mode width but also for avoiding additional loss, since, in practice, any structural irregularities would result in coupling of waveguide modes (especially those close to the cutoff) to plane SPPs propagating away from the waveguide and thereby result in additional propagation loss.

Acknowledgments

The authors acknowledge the support by the European Network of Excellence, PLASMO-NANO-DEVICES (FP6-2002-IST-1-507879), the Danish Agency for Science, Technology and Innovation (contract No. 274-07-0258), and from the NABIIT project financed by the Danish Research Agency (contract No. 2106-05-033).

#90643 - $15.00 USD Received 11 Dec 2007; revised 7 Feb 2008; accepted 7 Feb 2008; published 12 Feb 2008